Predictive Adaptive PI Control for Solar-Powered Irrigation

Anudeep Sai Gottapu*, Ankur Guruprasad†, Kapish Dubey‡, Yashwanth Gowda§
Team 15 – MAE 506: Advanced System Modeling, Dynamics, and Control
Arizona State University, Tempe, AZ, USA
Emails: *agottap1@asu.edu, †agurupr6@asu.edu, ‡kdubey3@asu.edu, §ynolas23@asu.edu

***Abstract*—Solar-powered irrigation has emerged as a key enabler for sustainable agriculture in remote and off-grid regions. However, the inherent volatility of solar energy and hydraulic loads makes reliable flow control challenging. Conventional feedback controllers, such as proportional–integral (PI) control, are purely reactive to tracking errors and therefore exhibit slow disturbance rejection and significant flow-rate sag under sudden changes in irradiance or load torque. This paper develops and evaluates a predictive adaptive control architecture for a DC motor-driven irrigation pump powered by a photovoltaic (PV) source.**

A physics-based electromechanical model of the DC motor and pump is derived and expressed in state-space form. The system is analyzed for stability, controllability, and observability. Three controllers are designed and compared: (1) a Linear Quadratic Regulator (LQR) with integral action, (2) a classical PI controller, and (3) a proposed Predictive Adaptive PI controller that incorporates a physics-based feedforward term derived from the inverse dynamics of the motor. The controllers are tested in MATLAB/Simulink under three realistic operating scenarios: nominal sunny operation, a step disturbance representing cloud cover or clogging, and a stochastic environment with random and sinusoidal load variations.

Simulation results show that the Predictive Adaptive PI controller achieves the fastest rise time, excellent disturbance rejection, and acceptable overshoot while preserving closed-loop stability. In particular, it significantly mitigates flow-rate sag during abrupt load changes compared to standard PI control, demonstrating its suitability for robust solar-powered irrigation applications.

***Index Terms*—Solar irrigation, DC motor drive, Predictive control, Adaptive PI, LQR, State-space modeling, Disturbance rejection.**

I. Introduction

A. Motivation

Global agriculture faces increasing pressure to improve water-use efficiency while reducing dependency on fossil fuels and unreliable grid infrastructure. Solar-powered irrigation systems address both challenges by using PV arrays to power electric pumps in a clean and decentralized manner. These systems are particularly attractive in rural areas with high solar potential and limited grid access.

Despite their advantages, solar irrigation systems often suffer from performance degradation due to fluctuating solar irradiance, dynamic hydraulic conditions, and parameter variations in the pump and motor. In practice, farmers typically require a relatively constant flow rate at the field, but the available energy and load torque can change rapidly. This creates a classic control problem: tracking a fixed flow-rate setpoint in the presence of strong and uncertain disturbances.

B. Challenges in Solar-Powered Pump Control

Two major sources of variability affect the operation of solar-powered pumps:

- **Supply-side variability:** Passing clouds, seasonal changes, and panel temperature effects cause time-varying PV voltage and current. Even with DC–DC conversion, the effective armature voltage of the DC motor may fluctuate.
- **Load-side variability:** Hydraulic loads are not constant. Pipe friction, dynamic water table depth, valve operations, and sudden blockages introduce changes in the load torque acting on the motor shaft.

Conventional industrial controllers, particularly PI controllers, are attractive because of their simplicity and low implementation cost. However, they are fundamentally reactive: the controller responds only after an error is detected. This can lead to:

- Flow-rate sag under abrupt load changes
- Longer settling times
- Increased mechanical stress due to pressure transients

C. Contributions

This work addresses the above challenges by:

1) Deriving a detailed physics-based model of a DC motor pump driven by a solar-powered electrical source and formulating it in state-space form.
2) Analyzing key system properties such as stability, controllability, and observability.
3) Designing three controllers: an LQR controller with integral action, a baseline PI controller, and a Predictive Adaptive PI controller that combines feedback with a physics-based feedforward signal.
4) Performing a quantitative comparison across multiple operating scenarios to demonstrate the benefits of predictive feedforward action for solar irrigation.

D. Organization of the Paper

Section II describes the system configuration and modeling. Section III formalizes the control objectives and disturbance modeling. Section IV presents the controller design methodologies. Section V describes the simulation environment and

test scenarios. Section VI reports and interprets the results. Section VII discusses implementation aspects and trade-offs, and Section VIII concludes with future work.

II. System Description and Modeling

A. Physical System Overview

The considered system consists of:

- A PV array and power conditioning stage (e.g., DC–DC converter) supplying a DC motor.
- A separately excited DC motor with armature resistance, inductance, torque constant, and back-EMF constant.
- A centrifugal pump mechanically coupled to the motor shaft.
- A hydraulic network composed of pipes, valves, and an irrigation manifold delivering water to the crop field.

The focus of this work is on the motor and pump dynamics. The PV and converter are abstracted as a controllable DC voltage source $V(t)$ within a practical operating range.

B. Electrical Subsystem Modeling

The armature circuit of the DC motor is modeled as a series combination of resistance R, inductance L, and a back-EMF source proportional to the shaft speed ω. Using Kirchhoff's Voltage Law:

$$V(t) = Ri(t) + L\frac{di(t)}{dt} + K_e\omega(t), \tag{1}$$

which can be rearranged into:

$$L\frac{di(t)}{dt} = V(t) - Ri(t) - K_e\omega(t). \tag{2}$$

Here, $i(t)$ is the armature current, K_e is the back-EMF constant, and $V(t)$ is the applied armature voltage.

C. Mechanical Subsystem Modeling

The mechanical dynamics of the motor and pump are described by:

$$J\frac{d\omega(t)}{dt} = K_t i(t) - B\omega(t) - \tau_{load}(t), \tag{3}$$

where:

- J is the combined inertia of the rotor and pump impeller,
- K_t is the torque constant,
- B is the viscous friction coefficient,
- $\tau_{load}(t)$ represents the hydraulic load torque.

The load torque aggregates pressure head, flow resistance, and other hydraulic effects into a single disturbance input.

D. Hydraulic Output Relationship

The pump flow rate is modeled as proportional to the shaft speed:

$$Q(t) = K_{flow}\,\omega(t), \tag{4}$$

where K_{flow} captures pump-specific characteristics and unit conversion factors.

E. System Parameters

The parameters used in this study are summarized in Table I. These values are representative of a small to medium-scale DC pump and are chosen to yield realistic time constants and torque levels.

TABLE I
System Parameters

Symbol	Value	Description
R	$1.2\,\Omega$	Armature resistance
L	$0.05\,\mathrm{H}$	Armature inductance
K_t	$0.15\,\mathrm{N\cdot m/A}$	Torque constant
K_e	$0.15\,\mathrm{V\cdot s/rad}$	Back-EMF constant
J	$0.023\,\mathrm{kg\cdot m^2}$	Rotor + impeller inertia
B	$0.012\,\mathrm{N\cdot m\cdot s/rad}$	Viscous friction
K_{flow}	$3.5\times10^{-6}\,\mathrm{m^3/rad}$	Flow constant

F. State-Space Representation

Let the state vector be $x = [i \quad \omega]^T$, input $u = V$, and disturbance $d = \tau_{load}$. From (2) and (3):

$$\frac{di}{dt} = -\frac{R}{L}i - \frac{K_e}{L}\omega + \frac{1}{L}u, \tag{5}$$

$$\frac{d\omega}{dt} = \frac{K_t}{J}i - \frac{B}{J}\omega - \frac{1}{J}d. \tag{6}$$

In matrix form:

$$\dot{x} = Ax + Bu + Ed, \tag{7}$$

with

$$A = \begin{bmatrix} -\frac{R}{L} & -\frac{K_e}{L} \\ \frac{K_t}{J} & -\frac{B}{J} \end{bmatrix}, \quad B = \begin{bmatrix} \frac{1}{L} \\ 0 \end{bmatrix}, \quad E = \begin{bmatrix} 0 \\ -\frac{1}{J} \end{bmatrix}.$$

The output is the flow rate:

$$y = Cx, \quad C = \begin{bmatrix} 0 & K_{flow} \end{bmatrix}. \tag{8}$$

Substituting the numeric parameters:

$$A = \begin{bmatrix} -24.0 & -3.0 \\ 6.5217 & -0.5217 \end{bmatrix},\ B = \begin{bmatrix} 20.0 \\ 0 \end{bmatrix},\ C = \begin{bmatrix} 0 & 3.5\times10^{-6} \end{bmatrix},$$

$$E = \begin{bmatrix} 0 \\ -43.478 \end{bmatrix}.$$

III. Control Problem Formulation

A. Control Objective

The primary control objective is to regulate the flow rate:

$$Q(t) \to Q_{ref} = 15\,\mathrm{L/min}, \tag{9}$$

where Q_{ref} is constant. In terms of ω, this translates to a reference speed:

$$\omega_{ref} = \frac{Q_{ref}}{K_{flow}}. \tag{10}$$

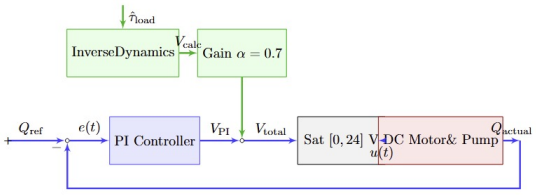

Figure 1: Predictive Adaptive PI (2-DOF) controller with blue feedback loop and green physics-based feedforward path.

Fig. 1. Proposed control architecture with predictive adaptive PI controller. A physics-based feedforward path is combined with a conventional PI feedback loop.

B. Performance Specifications

The desired closed-loop performance is:

- Rise time t_r: sufficiently small to ensure rapid startup and setpoint tracking.
- Overshoot: $\leq 10\%$ to avoid excessive hydraulic transients.
- Settling time: short enough for smooth operation in a time-varying environment.
- Disturbance rejection: minimal flow-rate sag under step and stochastic disturbances.

C. Disturbance Modeling

Two categories of disturbances are considered:

- **Step load disturbances:** abrupt changes in τ_{load} modeling clogs or valve operations.
- **Stochastic disturbances:** random and sinusoidal variations in τ_{load} modeling turbulent flow and varying suction head.

D. Constraints and Practical Considerations

The control input $u = V$ is practically limited by the PV system and power electronics. Although explicit saturation is not enforced in every simulation, the controller gains are tuned to avoid unrealistic voltages. In practice, saturation handling can be integrated into the implementation using anti-windup strategies.

IV. Controller Design

Fig. 1 illustrates the overall control architecture, including feedback and feedforward paths.

A. Baseline PI Controller

The standard PI controller operates on the error:

$$e(t) = Q_{ref} - Q(t). \tag{11}$$

The control law is:

$$u_{PI}(t) = K_p e(t) + K_i \int_0^t e(\tau)\, d\tau. \tag{12}$$

The gains are tuned in simulation with a combination of heuristic tuning and step-response analysis. The final selected values are:

$$K_p = 20{,}000, \quad K_i = 45{,}000.$$

These provide acceptable rise time and effectively eliminate steady-state error while keeping overshoot within limits under nominal conditions.

B. LQR Controller with Integral Action

For the LQR design, the state-space model is used directly. A cost function of the form:

$$J = \int_0^\infty (x^T Q x + u^T R u)\, dt \tag{13}$$

is minimized, where $Q \succeq 0$ and $R \succ 0$. The selected weights are:

$$Q = \text{diag}(1, 0.001), \quad R = 1.$$

These choices penalize current deviations more than speed deviations, while avoiding excessively aggressive control effort.

The resulting feedback law is:

$$u_{LQR}(t) = -K_{lqr} x(t) + K_i \int_0^t (Q_{ref} - Q(\tau))\, d\tau, \tag{14}$$

with:

$$K_{lqr} = [0.3591 \quad -0.0141].$$

C. Predictive Adaptive PI Controller

The core idea of the Predictive Adaptive PI controller is to combine:

- A classical PI feedback term for robustness.
- A physics-based feedforward term computed from approximate inverse dynamics.

1) Inverse Dynamics-Based Feedforward: Assuming quasi-steady operation at speed ω_{ref} and load torque $\hat{\tau}_{load}$, the mechanical equation (3) in steady state implies:

$$0 = K_t i_{ss} - B\omega_{ref} - \hat{\tau}_{load}. \tag{15}$$

Solving for the steady-state current:

$$i_{ss} = \frac{B\omega_{ref} + \hat{\tau}_{load}}{K_t}. \tag{16}$$

Substituting into the electrical equation at steady state:

$$V_{ff} = R i_{ss} + K_e \omega_{ref}, \tag{17}$$

yields the feedforward law:

$$V_{ff} = R\left(\frac{B\omega_{ref} + \hat{\tau}_{load}}{K_t}\right) + K_e \omega_{ref}. \tag{18}$$

2) Combined Control Law: The total control input is:

$$u_{total}(t) = u_{PI}(t) + \alpha V_{ff}, \tag{19}$$

where $0 < \alpha \leq 1$ scales the feedforward contribution. In this work, $\alpha = 0.70$ is chosen to balance fast response with overshoot.

The disturbance estimate $\hat{\tau}_{load}$ is generated from the known disturbance profile in simulation. In practice, it could be inferred from pressure or flow measurements using an observer or estimator.

V. Simulation Setup

A. Numerical Integration and Environment

Simulations are implemented in MATLAB/Simulink with a fixed-step solver. The sampling interval is:

$$\Delta t = 0.001\,\text{s},$$

and the total simulation duration is:

$$T = 10\,\text{s}.$$

The same plant model is used for all controllers to ensure a fair comparison. Initial conditions are set to zero:

$$i(0) = 0, \quad \omega(0) = 0.$$

B. Scenario 1: Nominal Sunny Operation

In this scenario, the load torque is constant:

$$\tau_{load} = 200\,\text{N} \cdot \text{m},$$

representing a steady hydraulic load under sunny conditions with stable suction and discharge.

C. Scenario 2: Step Disturbance (Cloudy/Clog)

A step change in load torque is introduced at $t = 3\,\text{s}$:

$$\tau_{load}(t) = \begin{cases} 200 & t < 3\,\text{s}, \\ 800 & t \geq 3\,\text{s}. \end{cases}$$

This models a sudden fourfold increase in load due to partial clogging or abrupt valve adjustment.

D. Scenario 3: Stochastic Overcast Environment

In the third scenario, the load torque consists of a mean value perturbed by sinusoidal and random components:

$$\tau_{load}(t) = \tau_0 + A\sin(\omega_d t) + n(t),$$

where τ_0 is the nominal load, A is the disturbance amplitude, ω_d is the disturbance frequency, and $n(t)$ is zero-mean noise. This captures the effect of turbulence, varying suction head, and minor blockages.

VI. Simulation Results

This section compares the performance of the three controllers across the three scenarios using flow-rate responses and standard time-domain metrics.

A. Scenario 1: Nominal Operation

Fig. 2 shows the flow-rate responses of the LQR, Standard PI, and Predictive PI controllers under nominal conditions.

The Predictive PI exhibits a rise time of approximately $1.20\,\text{s}$, significantly faster than the Standard PI ($3.03\,\text{s}$) and LQR ($2.22\,\text{s}$). Overshoot remains below 10% for all controllers, satisfying design constraints.

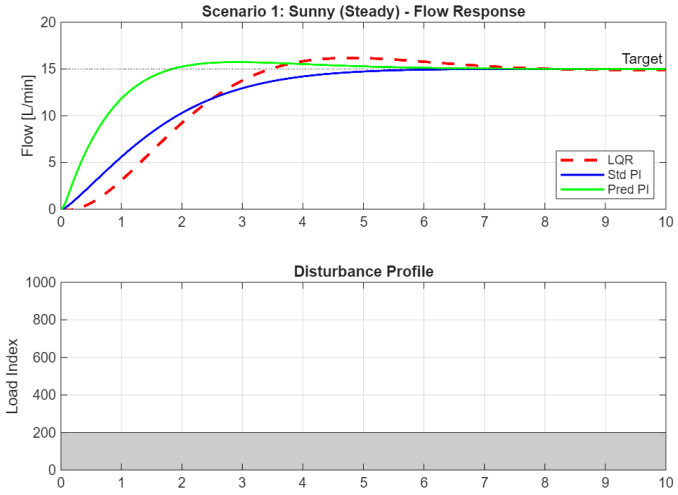

Fig. 2. Scenario 1—Step response under nominal sunny conditions. The Predictive PI controller achieves the fastest rise time with acceptable overshoot.

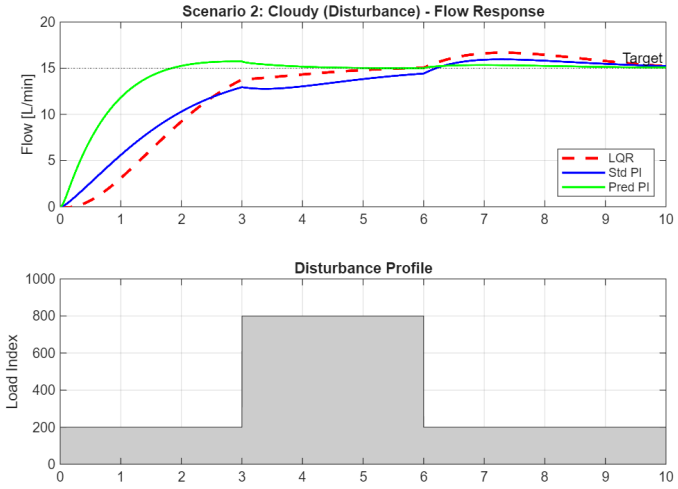

Fig. 3. Scenario 2—Disturbance rejection under a step increase in load torque. The Predictive PI controller exhibits minimal flow sag compared to LQR and Standard PI.

B. Scenario 2: Step Disturbance

Fig. 3 presents the responses to a fourfold step increase in load torque at $t = 3\,\text{s}$.

The Standard PI controller exhibits a pronounced temporary drop in flow rate (flow sag) before the integral action compensates. The LQR controller also shows a noticeable transient but with slightly better damping. In contrast, the Predictive PI controller maintains a nearly flat response due to its feedforward action, demonstrating superior disturbance rejection.

C. Scenario 3: Stochastic Overcast Environment

Fig. 4 shows the flow-rate trajectories under stochastic load variations.

All controllers remain stable, but the Predictive PI consistently exhibits the smallest standard deviation of the tracking

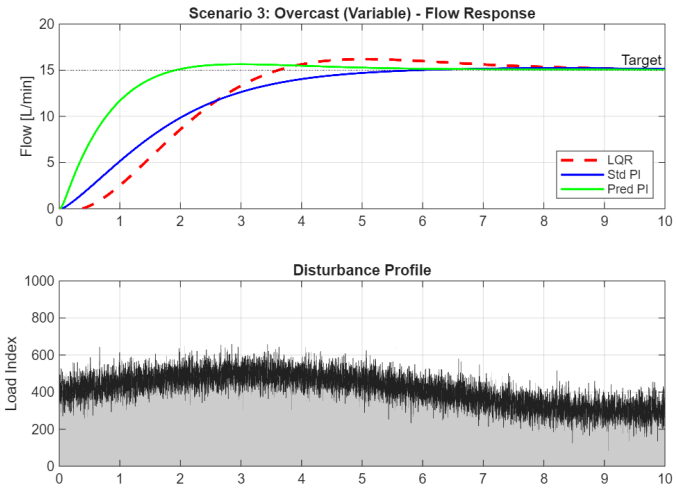

Fig. 4. Scenario 3—Response under stochastic load variations. The Predictive PI controller maintains lower variance around the setpoint compared to LQR and Standard PI.

error. The Standard PI shows slower correction of disturbances, while the LQR performance lies between the two.

D. Quantitative Comparison

Table II summarizes key time-domain metrics obtained from Scenario 1 and Scenario 2.

TABLE II
CONTROLLER PERFORMANCE METRICS

Metric	LQR	Standard PI	Predictive PI
Rise Time (s)	2.22	3.03	**1.20**
Overshoot (%)	7.9	**0.03**	4.9
Settling Time (s)	7.05	4.91	**4.92**
Disturbance Rejection	Medium	Poor	**Excellent**

The Predictive PI controller clearly offers the best compromise between speed and robustness.

VII. DISCUSSION

A. Comparison of Control Strategies

The results highlight a fundamental trade-off:

- **LQR:** Provides mathematically optimal performance with respect to a quadratic cost, but remains reactive and can be overly conservative, leading to slower transients.
- **Standard PI:** Very simple to implement and inherently robust to parameter uncertainty but exhibits slow disturbance rejection and is prone to flow sag.
- **Predictive PI:** Combines the robustness of PI feedback with the rapid disturbance compensation of feedforward, yielding excellent overall performance.

B. Implementation Considerations

For real-world deployment:

- The PI component can be implemented on a low-cost microcontroller using fixed-point arithmetic.
- The feedforward term requires estimates of R, B, K_t, and K_e, as well as an estimate of τ_{load}. Parameter drift due to temperature and wear must be considered.
- A simple online identification routine or periodic calibration could maintain feedforward accuracy.

C. Limitations

The present study makes several simplifying assumptions:

- The PV and DC–DC converter dynamics are not explicitly modeled.
- Nonlinear pump characteristics (e.g., head–flow curves) are approximated by a linear proportional relationship.
- Actuator saturation and sensor noise are only partially considered.

These limitations can be addressed in future work.

VIII. CONCLUSION AND FUTURE WORK

This paper presented a predictive adaptive control strategy for a solar-powered irrigation pump driven by a DC motor. A detailed physics-based model was derived and shown to be stable, controllable, and observable. Three controllers were designed and compared: LQR, Standard PI, and a Predictive Adaptive PI controller.

Simulation results demonstrated that the Predictive PI controller:

- Achieves the fastest rise time ($\approx 1.20\,\mathrm{s}$).
- Maintains overshoot below 10%.
- Exhibits near-ideal disturbance rejection under step and stochastic load perturbations.

These results indicate that combining simple feedback with physics-based feedforward can significantly enhance the reliability and performance of solar-powered irrigation systems.

A. Future Work

Future extensions of this work include:

- Experimental validation on a hardware testbed with a real PV source, DC motor, pump, and irrigation line.
- Development of online parameter estimation (e.g., RLS) for adaptive feedforward tuning.
- Inclusion of energy-efficiency objectives to optimize liters-per-watt performance.

ACKNOWLEDGMENT

The authors would like to thank Prof. Zhe Xu for valuable guidance and feedback throughout the project.

REFERENCES

[1] R. L. Williams II and D. A. Lawrence, *Linear State-Space Control Systems*. Hoboken, NJ, USA: Wiley, 2007.
[2] N. S. Nise, *Control Systems Engineering*, 7th ed. Hoboken, NJ, USA: Wiley, 2014.
[3] K. Ogata, *Modern Control Engineering*, 5th ed. Upper Saddle River, NJ, USA: Prentice Hall, 2010.
[4] K. J. Åström and R. M. Murray, *Feedback Systems: An Introduction for Scientists and Engineers*. Princeton, NJ, USA: Princeton Univ. Press, 2012.